

Electrochemical & Thermal Analysis of the Thermal Battery

Jang Hyeon Cho, Byeong June Park, Ji Youn Kim, Sang-Hyeon Ha, Chae Nam Im

The 4th R&D Institute-4, Agency for Defense Development, Daejeon 305-600, Korea

jhcho4535@naver.com / 82-10-5050-4539

Abstract: Both heat source exothermic reaction and discharge resistance(joule heat) are the most detrimental failure causes of thermal batteries. To avoid thermal runaway and explosion of the thermal battery, battery manufacturers rely heavily on repetitive and empirical trial-error methods for the battery component design. ADD has developed innovative simulation technology with the function of electrochemical & thermal analysis for the high temperature thermal batteries. This analysis technology is based on the commercial program 'COMSOL Multiphysics' that is efficient in the field of reciprocal electrochemistry and heat transfer analysis, etc. This paper provides electrochemical & thermal analysis results on the thermal batteries with various heat source thickness. This analytical results would be useful for the design of electrodes, electrolytes, heat sources, insulator and the other components. Additionally, this 'COMSOL' program analysis method could be applied to pure lithium typed thermal batteries, lithium-ion batteries and packages.

Keywords: thermal battery, electrochemical & thermal analysis, COMSOL, thermal design

Introduction

Thermal batteries for precision weapon system must be met stringent requirements such as high power, high energy density, long shelf-life and severe environmental conditions, etc.

These requirements of thermal batteries are mainly determined by the electrolyte(eutectic salts) which has excellent ionic conductivity at high temperatures(above 500 °C) but almost non-conductive at room temperature.

Once ignited, the temperature of a thermal battery rises above the electrolyte melting point owing to the internal heat source. As a result, the thermal battery exhibits high power density.

When the heat source is activated by the igniter, the internal temperature of a thermal battery is getting increased by the exothermic reaction of the heat source(Fe/KClO₄). Here, Fe/KClO₄ is the main exothermic material and the most detrimental failure causes of thermal batteries.

As the ion conductivity of the electrolyte increases with rising temperature, the performance of the thermal battery is influenced by the temperature of various components inside the cell stack. Figure 1 shows the reaction concept of thermal battery(unit cell).

In general, the thermal battery is composed of anode(Li-Si alloy), electrolyte(LiCl-LiBr-LiF salt), cathode(FeS₂) and heat source.

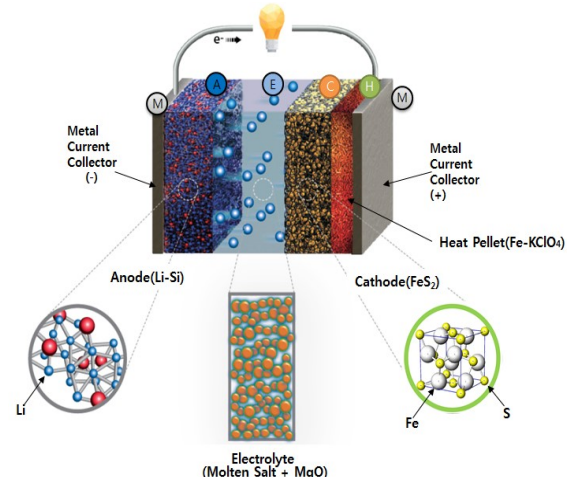


Figure 1. Concept of thermal battery(unit cell)

The electrolyte has the melting point of about 430°C. The decomposition temperature of the cathode FeS₂ varies depending on the condition such as particle size and shape, nevertheless is nearly about 550°C. For this reason, it is crucial to maintain the temperature of about 500~550°C for optimal performance of the thermal battery. Figure 2 shows the thermal runaway of thermal batteries.



Figure 2. Thermal runaway of thermal batteries

However, practically, all of unit cells in the thermal battery do not have the uniform temperature distribution due to shape, component arrangement and heat transfer effect. After all, it has different temperature distribution depending on where the unit cell is located and how the discharge time is elapsed. Therefore, the performance estimation obtained by unit cell testing at constant temperature conditions may differs from actual cell stacks.

Until now, the performance predictions of thermal battery has been performed mainly using SIMULINK and Lump Model. However, it seems that this model did not seem to have helped optimize the thermal battery design.

Therefore, in this study, the performance prediction of thermal batteries using 'COMSOL Multiphysics' is executed. 'COMSOL Multiphysics' program has both an electrochemical model and a heat transfer analysis function.

Unit cell test

Prior to the performance prediction of a thermal battery, the unit cell discharge experiment was performed under various temperature conditions. The unit cell test equipment is shown in Figure 3.

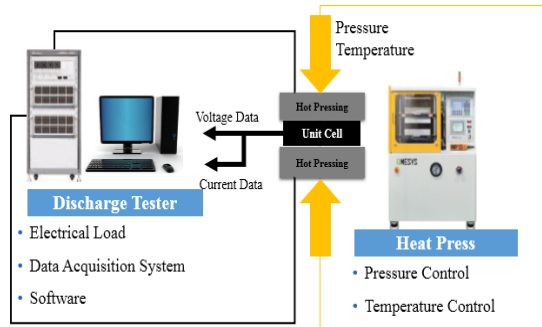


Figure 3. Unit Cell Discharge Test System

Thermal battery is composed of various components such as anode, cathode, electrolyte, heat source, insulator, igniter, case and so on. But, for unit cell testing, only cathode, anode and electrolyte are used. Table 1 shows the physical properties of electrodes and electrolyte constituting the unit cell, all pellets were formed by cold pressing.

Table 1. Materials of unit cell

Material	Mass (g)	O.D (mm)	I.D (mm)	Thickness (mm)
Cathode (FeS ₂)	1.81	44.67	8.32	0.38
Electrolyte (AlLi-Li)	1.48	44.92	7.56	0.4
Anode (Li-Si alloy)	1.14	44.74	8.47	0.67

The experimental conditions are shown in Table 2.

Table 2. Unit cell discharge test cases(51 cases)

Test conditions			
Temperature(°C)			430°C ~ 590°C (10°C interval)
Current(A) (Repetition profile)	7.6 A/2.4 s, 0 A/0.1 s	15.1A/2.4 s, 0A/0.1s	22.7A/2.4 s, 0A/0.1 s

When the temperature of the press is reached at setting point as shown in Figure 3, a unit cell was inserted between the upper plate and the lower plate, pressed to 250kg, and then

was maintained for 2 minutes. Then, the stepwise discharge was performed according to the above Table 2.

The formula for calculating internal resistance of a unit cell is shown in Equation(1) published by Fujiwara et al., V_{ocv} is based on the voltage at 0.03 second after applying 0A and V_{ccv} is the voltage at 0.01 second after 0A discharge.

$$R_{tot} = \frac{V_{ocv} - V_{ccv}}{I_{ccv}} \dots (1)$$

The internal resistance is calculated using applied current values(I_{ccv}). The results of a unit cell discharge test($0.5\text{A}/\text{cm}^2$, $1.0\text{A}/\text{cm}^2$, $1.5\text{A}/\text{cm}^2$) are shown in Figures 4, 5 and 6.

As the result of a unit cell discharge, it can be seen that the internal resistance of unit cell is very high when the temperature is less than 450°C . The reason is that viscosity of the electrolyte is too low and the conductivity is greatly lowered.

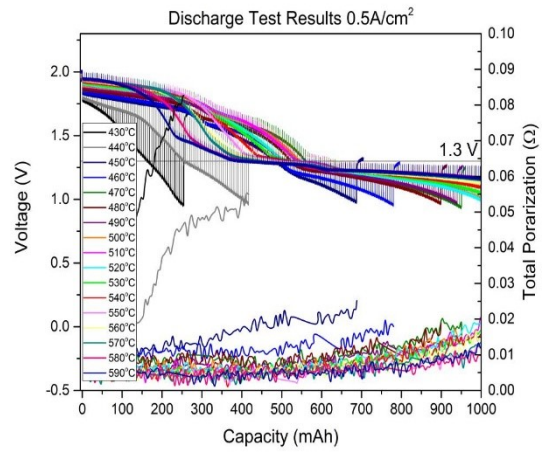


Figure 4. Unit cell discharge results ($0.5\text{A}/\text{cm}^2$)

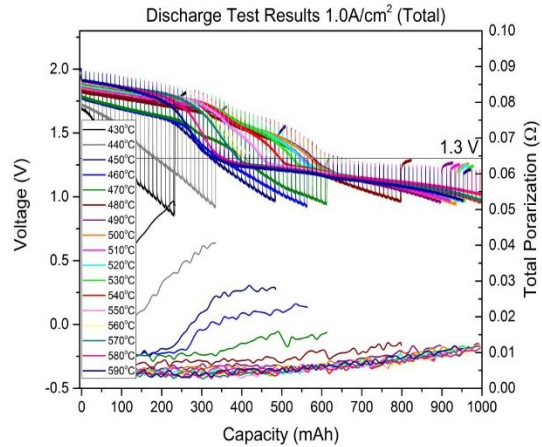


Figure 5. Unit cell discharge results ($1.0\text{A}/\text{cm}^2$)

Figure 7 shows the analysis results of the above discharge conditions($0.5\text{A}/\text{cm}^2$, $1.0\text{A}/\text{cm}^2$, $1.5\text{A}/\text{cm}^2$).

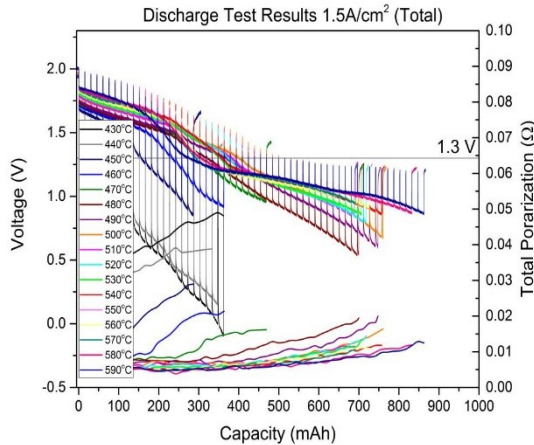


Figure 6. Unit cell discharge results ($1.5\text{A}/\text{cm}^2$)

Although there is a slight difference depending on the discharge rate, the optimal temperature range of a thermal battery is about $480\text{--}540^\circ\text{C}$.

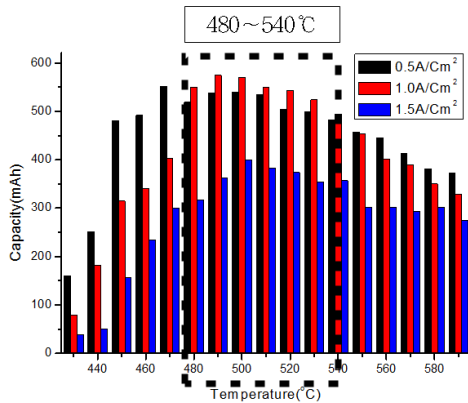


Figure 7. Unit cell discharge capacity results.

Thermal analysis of thermal battery

For optimal capacity of the thermal battery, the amount of the heat source must be carefully determined. If the amount of heat source in the thermal battery is too much, it may cause to overheat and rupture. On the other hand, if the amount of the heat source is too little, it is difficult to expect an optimum output because of low temperature.

In order to determine the amount of heat source for maintaining the optimal internal temperature of a thermal battery. The heat transfer & distribution inside the thermal battery was estimated using COMSOL program.

The component values and geometric shape for modeling is as Table 3 and Figure 8. The thickness of heat source are range from $0.8\text{mm}\text{--}1.5\text{mm}$.

As shown in Figure 8, the temperature measurement points inside thermal battery are set at the middle of the cell stack(#4rd cell, red circle), cathode / electrolyte / anode /

collector / heat source of #1st cell(dot line), insulator and cell case(red circle).

Table 3. Physical properties of a battery components.

Material	O.D (mm)	Density (g/cm ³)	Thickness (mm)
Cathode (FeS_2)	55.87	2.783	0.710
Electrolyte (AlLi)	56.24	2.240	0.430
Anode (Li-Si alloy)	56.08	1.060	1.000
Heat source (Fe/KClO_4)	56.17	3.300	0.8/0.9/1.0/1.2/1.5
Insulator (BF paper)		8.908	Ref. Figure 8
Case (SUS304)			Ref. Figure 8

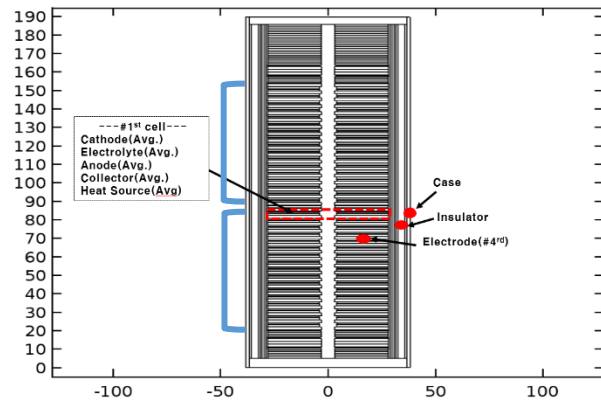


Figure 8. Temperature measurement point of thermal battery.

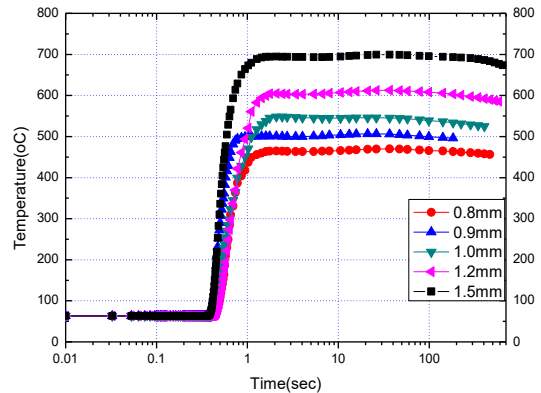


Figure 9. Temperature profiles of the #4th electrode of thermal battery(at $0.8\text{--}1.5\text{mm}$ heat source thickness)

Thermal analysis results

Through COMSOL program simulation, it was found that the temperature of electrode(#4rd) of a thermal battery differs according to the amount of heat source. As figure 7 shown,

in the case 1.5mm thickness of heat source, the temperature of electrode rises up to 700°C. On the other hand, at 0.7mm, it was maintained at 460°C.

The optimal discharge performance was achieved when the thickness of heat source is 0.9~1.0mm. The rising time up to the temperature for optimal performance is about 1.0 sec. Figure 10 shows the average temperature of #1st cell vs. time. Here, #1st cell is located in the center of stack.

The highest average temperature of the heat source is 900°C (figure 10), but peak temperature reaches up to 1300°C at 0.2 second (figure 11).

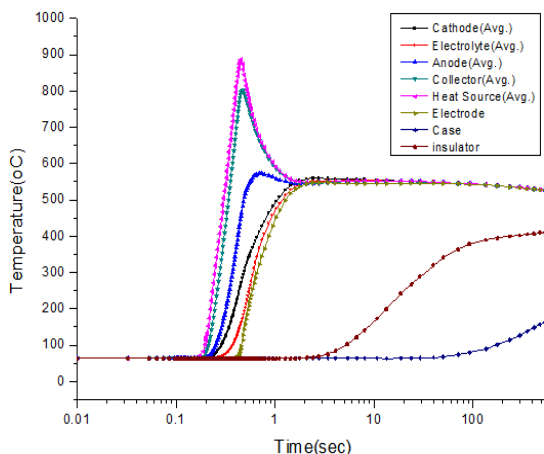


Figure 10. Temperature profiles of thermal battery components(at 1.0mm heat source thickness).

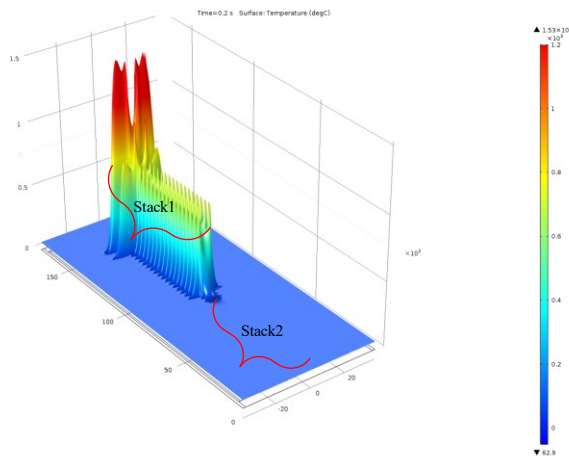


Figure 11. Temperature profiles of thermal battery components(0.2sec, at heat source 1.0mm, 45° view).

At the elapse of 10 seconds after the ignition, temperature profiles of thermal battery is as figure 12. The each side temperature of thermal battery reached above 800°C and that of central parts was up to about 600°C owing to the amount of dense heat source. The temperatures of stack1 and stack2 are maintained about 500~550°C.

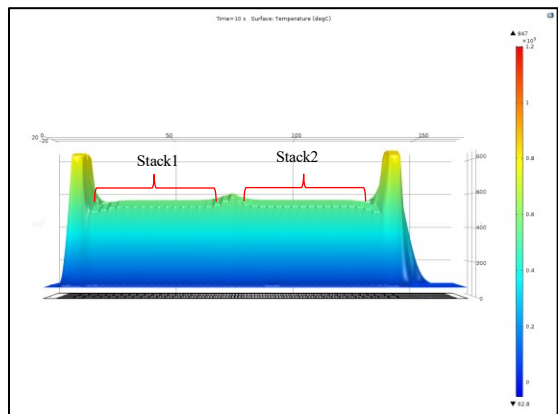


Figure 12. Temperature profiles of thermal battery components(10sec, at heat source 1.0mm, front view).

Acknowledgements

The authors wish to thank Sueng Soo Baek(ADD 44th Directorate) and electric power source team members of ADD. Also authors gratefully acknowledge funding from ADD defense S&T programs.

References

1. Seung Ho Kang, Ph.D Dissertation, 161, 1443 (2006).
2. H. W. Cheong, S. H. Kang, J. M. Kim, and S. B. Cho, Journal of Ceramic Processing Research, 13, 198 (2012).
3. Y. S. Choi, H. R. Yu, H. W. Cheong, S. B. Cho and Y. S. Lee, Appl. Chem. Eng. 25, 2, 161-166 (2014).
4. Freitas, C. S. Giancarlo, C. P. Fernando, and S. V. Ardson, Journal of Power Sources, 179.1, 424-429 (2008)
5. R. A. Guidotti, P. Masset, Journal of Power Sources, 183, 388-398 (2008)
6. H. J. Ji, Journal of the Korea Institute of Military Science and Technology, 11(1), 102-111 (2008)
7. S. Fujiwara, M. Inaba, and A. Tasaka, Journal of Power Sources, 196(8), 4012-4018 (2011)
8. A. G. Bergman, A. S. Arabadshan, Russ. J. Inorg. Chem. (English Trans.), 8(5), 369 (1963)
9. R. A. Guidotti, F. W. Reinhardt, Proceedings of the 33rd International Power Sources Conference, 369 (1988)
10. P. Masset, PhD Thesis, National Polytechnic Institute of Grenoble, Grenoble (2002)
11. J. R. Selman, D. K. DeNuccio, C. J. Sy, R. K. Steunenberg, Journal of Electrochemical Society, 124(8), 1160 (1977)
12. Y. S. Choi, H. R. Yu, H. W. Cheong, S. B. Cho and Y. S. Lee, Appl. Chem. Eng. 25, 1, 72-77 (2014).
13. S. Schoeffert, Journal of Power Sources, 142, 361-369 (2005)
14. S. Schoeffert, 40th Power Sources Conference, Cherry Hill-USA, June (2002).